

IMAGE SEGMENTATION AND TOTAL VARIATION DENOISING

*Erkut Erdem**

Hacettepe University

March 15th, 2013

CONTENTS

1 Mumford-Shah (MS) Functional	1
2 Ambrosio-Tortorelli (AT) Approximation of the MS Functional	2
3 A Common Framework for Curve Evolution, Segmentation and Anisotropic Diffusion	6
4 Active Contours Without Edges	7
References	10

1 MUMFORD-SHAH (MS) FUNCTIONAL

The formulation of Mumford and Shah [6] is based on a functional minimization via which a piecewise smooth approximation of a given image and an edge set are to be recovered simultaneously. In this unified formulation, smoothing and edge detection processes work jointly to partition an image into segments. The Mumford-Shah (MS) model is:

$$(1) \quad E_{MS}(u, \Gamma) = \beta \int_{\Omega} (u - f)^2 dx + \alpha \int_{\Omega \setminus \Gamma} |\nabla u|^2 dx + length(\Gamma)$$

where

- $\Omega \subset \mathbb{R}^2$ is connected, bounded, open subset representing the image domain,
- f is an image defined on Ω ,
- $\Gamma \subset \Omega$ is the edge set segmenting Ω ,
- u is the piecewise smooth approximation of f ,
- $\alpha, \beta > 0$ are the scale space parameters of the model.

*erkut@cs.hacettepe.edu.tr

The first term in E_{MS} is the *data fidelity* term which forces u to be close to the original image f . The next two terms are the generic priors that provide certain knowledge about the solution. Specifically, the second term, the so-called *regularization* or *smoothness* term, gives preference to piecewise smooth images by penalizing high gradients. Since the integral is over $\Omega \setminus \Gamma$, this prior is turned off at image boundaries, and thus it excludes image edges to be smoothed out. The third term is a penalty term on total edge length which prevents the image to be split into many regions. Additionally, it implicitly imposes smoothness of the boundaries.

Generally, the unknown edge set Γ of a lower dimension makes the minimization of the MS model very difficult. Hence, in literature several approaches for approximating the MS model are suggested [1, 4]. In the next section, the approximation proposed by Ambrosio and Tortorelli [1] will be reviewed.

2 AMBROSIO-TORTORELLI (AT) APPROXIMATION OF THE MS FUNCTIONAL

Ambrosio and Tortorelli [1] suggested an approximation for the MS model by following the Γ convergence framework [2]. The basic idea is to introduce a smooth edge indicator function v which is more convenient than using the characteristic function χ_Γ as the edge indicator. The new function v depends on a parameter ρ , and as $\rho \rightarrow 0$, $v \rightarrow 1 - \chi_\Gamma$. That is, $v(x) \approx 0$ if $x \in \Gamma$ and $v(x) \approx 1$ otherwise. The result is the functional

$$(2) \quad E_{AT}(u, v) = \int_{\Omega} \left(\beta(u - f)^2 + \alpha(v^2 |\nabla u|^2) + \frac{1}{2} \left(\rho |\nabla v|^2 + \frac{(1 - v)^2}{\rho} \right) \right) dx .$$

In the Ambrosio-Tortorelli (AT) model, the continuous function v encodes the boundary information. The value of v at a point can be interpreted as a measure of *boundaryness* where the low values indicate the edge points. That is, $v \approx 0$ along the boundaries and grows rapidly away from them. Thus, the function v may be thought as a blurred version of the edge set. The parameter ρ specifies the level of blurring (Figure 1), and as $\rho \rightarrow 0$, $\frac{1}{2} \int_{\Omega} \left(\rho |\nabla v|^2 + \frac{(1 - v)^2}{\rho} \right) dx$ approximates the cardinality of the edge set Γ .

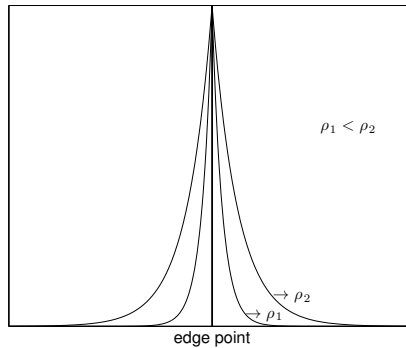


Figure 1: An example 1D edge strength function $(1 - v)$ for two different values of ρ .

Piecewise smooth image u and the edge strength function v are simultaneously computed via the solution of the following system of coupled PDEs:

$$(3) \quad \frac{\partial u}{\partial t} = \nabla \cdot (v^2 \nabla u) - \frac{\beta}{\alpha}(u - f); \quad \frac{\partial u}{\partial n} \Big|_{\partial\Omega} = 0,$$

$$(4) \quad \frac{\partial v}{\partial t} = \nabla^2 v - \frac{2\alpha|\nabla u|^2 v}{\rho} - \frac{(v-1)}{\rho^2}; \quad \frac{\partial v}{\partial n} \Big|_{\partial\Omega} = 0$$

where $\partial\Omega$ denotes the boundary of Ω and n denotes the outer unit normal vector to $\partial\Omega$.

Notice that PDE for each variable can be interpreted as a biased diffusion equation that minimizes a convex quadratic functional in which the other variable is kept fixed:

Keeping v fixed, Equation (3) minimizes a convex quadratic functional given by

$$(5) \quad \int_{\Omega} \left(\alpha v^2 |\nabla u|^2 + \beta (u - f)^2 \right) dx.$$

The data fidelity term in Equation (3) provides a bias that forces u to be close to the original image f . In the regularization term, the edge strength function v specifies the boundary points and guides the smoothing accordingly. Since $v \approx 0$ along the boundaries, no smoothing is carried out at the boundary points, thus the edges are preserved.

Keeping u fixed, Equation (4) minimizes a convex quadratic functional given by

$$(6) \quad \frac{\rho}{2} \int_{\Omega} \left(|\nabla v|^2 + \frac{1 + 2\alpha\rho|\nabla u|^2}{\rho^2} \left(v - \frac{1}{1 + 2\alpha\rho|\nabla u|^2} \right)^2 \right) dx.$$

The reciprocal relationship between v and $|\nabla u|^2$ can be clearly observed in the above functional. It asserts that the function v is nothing but a smoothing of $\frac{1}{1+2\alpha\rho|\nabla u|^2}$ with a blurring radius proportional to ρ and reciprocal to $|\nabla u|$. Ignoring the smoothness term $\rho|\nabla v|^2$, which mildly forces some spatial organization by requiring the edges to be smooth, and by letting $\rho \rightarrow 0$ [3, 9], $v \approx \frac{1}{1+2\alpha\rho|\nabla u|^2}$.

Considering this approximation and the relation between variational regularization and diffusion equations, Equation (3) can be interpreted as a Perona-Malik type nonlinear diffusion at a specific scale. Replacing v in Equation (3) with $1/(1 + 2\alpha\rho|\nabla u|^2)$ yields

$$(7) \quad \frac{\partial u}{\partial t} = \nabla \cdot (g(|\nabla u|) \nabla u) - \frac{\beta}{\alpha}(u - f)$$

where $g(|\nabla u|) = \left(\frac{1}{1+|\nabla u|^2/\lambda^2} \right)^2$ with $\lambda^2 = 1/(2\alpha\rho)$. Thus, $\sqrt{1/(2\alpha\rho)}$ can be seen as a contrast parameter.

Since the parameters α and β define the relative importance of the regularization term, the scale is determined by the ratio α/β . Keeping the value of α fixed, decreasing the value of β results in more simplified results (Figure 2(b)-(c)). Moreover, the scale space parameters α and β also define the detail level in segmentation. With the ratio α/β fixed, the level of detail increases with the increasing α (Figure 2(b)-(d)).



(a)



(b)



(c)



(d)

Figure 2: Example segmentation results (u and $1 - v$). (a) Source image. (b)-(d) Corresponding segmentations obtained with the parameters (b) $\alpha = 1$, $\beta = 0.01$, $\rho = 0.01$, (c) $\alpha = 1$, $\beta = 0.001$, $\rho = 0.01$, and (d) $\alpha = 4$, $\beta = 0.04$, $\rho = 0.01$, respectively.

Numerical Implementation

Equations (3) and (4) can be simultaneously solved for u and v using standard numerical discretization techniques such as finite differences. The coupled system is first discretized with respect to spatial variables. This leads to the following space-discrete system of equations:

$$\begin{aligned}
 \frac{du_{i,j}}{dt} &= v_{i+\frac{1}{2},j}^2 \cdot (u_{i+1,j} - u_{i,j}) - v_{i-\frac{1}{2},j}^2 \cdot (u_{i,j} - u_{i-1,j}) \\
 &+ v_{i,j+\frac{1}{2}}^2 \cdot (u_{i,j+1} - u_{i,j}) - v_{i,j-\frac{1}{2}}^2 \cdot (u_{i,j} - u_{i,j-1}) \\
 &- \frac{\beta}{\alpha} (u_{i,j} - f_{i,j}) ,
 \end{aligned}
 \tag{8}$$

$$\begin{aligned}
 \frac{dv_{i,j}}{dt} &= v_{i+1,j} + v_{i-1,j} + v_{i,j+1} + v_{i,j-1} - 4v_{i,j} \\
 &- \frac{2\alpha |\nabla u_{i,j}|^2 v_{i,j}}{\rho} - \frac{(v_{i,j} - 1)}{\rho^2} .
 \end{aligned}
 \tag{9}$$

As in the discretization of the Perona-Malik equation, the diffusivities represented by the edge strength function v at mid-pixel points can be computed by taking averages over neighboring pixels:

$$\tag{10} \quad v_{i\pm\frac{1}{2},j} = \frac{v_{i\pm 1,j} + v_{i,j}}{2}, \quad v_{i,j\pm\frac{1}{2}} = \frac{v_{i,j\pm 1} + v_{i,j}}{2} .$$

The time derivatives in Equations (8) and (9) can be discretized using forward differences, where regularization terms and the bias terms on the right hand side of each equation are evaluated at times k and $k + 1$, respectively.

$$\begin{aligned}
 \frac{u_{i,j}^{k+1} - u_{i,j}^k}{\Delta t} &= \left(v_{i+\frac{1}{2},j}^k \right)^2 \cdot u_{i+1,j}^k + \left(v_{i-\frac{1}{2},j}^k \right)^2 \cdot u_{i-1,j}^k \\
 &+ \left(v_{i,j+\frac{1}{2}}^k \right)^2 \cdot u_{i,j+1}^k + \left(v_{i,j-\frac{1}{2}}^k \right)^2 \cdot u_{i,j-1}^k \\
 &- \left(\left(v_{i+\frac{1}{2},j}^k \right)^2 + \left(v_{i-\frac{1}{2},j}^k \right)^2 + \left(v_{i,j+\frac{1}{2}}^k \right)^2 + \left(v_{i,j-\frac{1}{2}}^k \right)^2 \right) \cdot u_{i,j}^k \\
 &- \frac{\beta}{\alpha} \left(u_{i,j}^{k+1} - f_{i,j} \right) ,
 \end{aligned}
 \tag{11}$$

$$\begin{aligned}
 \frac{v_{i,j}^{k+1} - v_{i,j}^k}{\Delta t} &= v_{i+1,j}^k + v_{i-1,j}^k + v_{i,j+1}^k + v_{i,j-1}^k - 4v_{i,j}^k \\
 &- \frac{\alpha \left(\left(u_{i+1,j}^k - u_{i-1,j}^k \right)^2 + \left(u_{i,j+1}^k - u_{i,j-1}^k \right)^2 \right) v_{i,j}^{k+1}}{2\rho} - \frac{(v_{i,j}^{k+1} - 1)}{\rho^2}
 \end{aligned}
 \tag{12}$$

where Δt denotes the time step.

Although the suggested scheme is neither fully explicit nor fully implicit, it still allows us to compute u^{k+1} and v^{k+1} by using forward recursion as in an explicit scheme. A numerical stopping criteria for the iterative scheme can be defined in the sense that the rate of change of u is less than a threshold (Algorithm 1).

Algorithm 1 Minimization of the Ambrosio-Tortorelli Model

- 1: Initialize the variables with $u^0 = f$, $v^0 = \frac{1}{1+2\alpha\rho|\nabla u^0|^2}$
 - 2: **for** $k = 0$ to $kmax$ **do**
 - 3: Solve Equation (11) for u^{k+1}
 - 4: **if** $|u^{k+1} - u^k| < \epsilon|u^k|$ **then**
 - 5: stop iterations
 - 6: **end if**
 - 7: Solve Equation (12) for v^{k+1}
 - 8: **end for**
-

3 A COMMON FRAMEWORK FOR CURVE EVOLUTION, SEGMENTATION AND ANISOTROPIC DIFFUSION

The key idea of the Ambrosio-Tortorelli approximation of the Mumford-Shah functional (Section 2) is to utilize a continuous edge strength function v . The value of v approaches to 0 at the object boundaries and grows rapidly as image gradients become small. In [9], Shah suggested a modification to the Ambrosio-Tortorelli model Equation (2), where the quadratic cost functions in both the data fidelity and the smoothing terms are replaced with L^1 -functions. The modified energy is:

$$(13) \quad E_S(u, v) = \int_{\Omega} \left(\beta |u - f| + \alpha v^2 |\nabla u| + \frac{1}{2} \left(\rho |\nabla v|^2 + \frac{(1-v)^2}{\rho} \right) \right) dx .$$

As $\rho \rightarrow 0$, this energy functional converges to the following functional:

$$(14) \quad E_{S2}(u, \Gamma) = \frac{\beta}{\alpha} \int_{\Omega} |u - f| dx + \int_{\Omega \setminus \Gamma} |\nabla u| dx + \int_{\Gamma} \frac{J_u}{1 + \alpha J_u} ds$$

with $J_u = |u^+ - u^-|$ indicating the jump in u across Γ . u^+ and u^- denote intensity values on two sides of Γ , respectively, and thus each boundary point is weighted according to its level of contrast.

Minimizing E_S corresponds to the gradient descent equations:

$$(15) \quad \frac{\partial u}{\partial t} = 2\nabla v \cdot \nabla u + v |\nabla u| \text{curv}(u) - \frac{\beta}{\alpha v} |\nabla u| \frac{(u-f)}{|u-f|}; \quad \frac{\partial u}{\partial n} \Big|_{\partial\Omega} = 0 ,$$

$$(16) \quad \frac{\partial v}{\partial t} = \nabla^2 v - \frac{2\alpha |\nabla u| v}{\rho} - \frac{(v-1)}{\rho^2}; \quad \frac{\partial v}{\partial n} \Big|_{\partial\Omega} = 0$$

with $\text{curv}(u) = \nabla \cdot \left(\frac{\nabla u}{|\nabla u|} \right)$.

The Equation (16) is very similar to the evolution equation of v Equation (4) in the AT model; only $|\nabla u|^2$ is replaced with $|\nabla u|$. The determining factor of the model is the new evolution equation of u Equation (15). Replacing L^2 -norms in both the data fidelity and the smoothness terms by their L^1 -norms generates shocks in u and thus object boundaries are recovered as actual discontinuities. As it can be clearly seen from Figure 3, the suggested smoothing process of u gives rise to more cartoon-like, piecewise constant images (these results are obtained by using a half-quadratic approx-

imation of Shah’s modified energy proposed in [5]). However, the robust norms utilized attract the image towards the cartoon limit and catch unintuitive regions such as the one at the man’s right shoulder and the ones on the floor. It is important to remark that the effect of the scale space parameters α and β on segmentation results is similar compared to the one in AT model (cf. Figure 2). The amount of smoothing is determined by the ratio α/β , and increasing the value of α while keeping α/β fixed leads to more detailed segmentations.

One of the underlying assumptions of the original MS model and AT approximation is that the filtered image varies from the observed image by Gaussian noise. Hence, when a source image is corrupted by impulse noise, the corresponding smoothing process produces inadequate results. However, replacing the L^2 -norm with the L^1 in the modified model yields to a robust data fidelity term that can cope with impulse noise. For example, consider the noisy image given in Figure 4(a), which is degraded with 5% salt and pepper noise. Figure 4(b) and (c) depict the outcomes of the AT approximation and the modified model, respectively. As they demonstrate, the modified model eliminates the impulse noise during smoothing, however, noise still present in the AT result.

4 ACTIVE CONTOURS WITHOUT EDGES

Chan and Vese [4] proposed an approximation for the MS segmentation model by following the level-set based curve evolution formulation [7, 8]. Level sets provide an implicit contour representation where an evolving curve is represented with the zero-level line of a level set function (Figure 5). The basic aim of Chan and Vese (CV) model is to partition a given image into two regions that are likely to correspond object and background regions by embedding the object boundary by the zero-level curve of a 3D level set function.

Let ϕ be a level set function. Then, the Chan-Vese functional is

$$\begin{aligned}
 E_{CV}(c_1, c_2, \phi) &= \lambda_1 \int_{\Omega} (f - c_1)^2 H(\phi) dx + \lambda_2 \int_{\Omega} (f - c_2)^2 (1 - H(\phi)) dx \\
 (17) \quad &+ \mu \int_{\Omega} |\nabla H(\phi)| dx
 \end{aligned}$$

where $\lambda_1, \lambda_2 > 0$ and $\mu \geq 0$ are fixed parameters. The length parameter μ can be interpreted as a scale parameter since it determines the relative importance of the length term. The possibility of detecting smaller objects/regions increases with decreasing μ .

The model represents the segmented image with the variables c_1, c_2 and $H(\phi)$, where $H(\phi)$ denotes the Heaviside function of the level set function ϕ defined by

$$(18) \quad H(z) = \begin{cases} 1 & \text{if } z \geq 0 \\ 0 & \text{if } z < 0. \end{cases}$$

The Heaviside function of the level set function, $H(\phi)$, specifies object and background regions in the observed image f , while the last term in (17), $\int_{\Omega} |\nabla H(\phi)|$, expresses the length of the object boundary. On top of that, the scalars c_1 and c_2 denote the average gray values of object and background regions indicated by $\phi \geq 0$



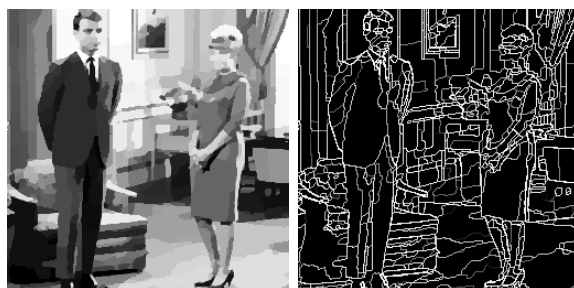
(a)



(b)



(c)



(d)

Figure 3: Example segmentation results (u and $1 - v$). (a) Source image. (b)-(d) Corresponding segmentations obtained with parameters (b) $\alpha = 1, \beta = 0.01, \rho = 0.01$, (c) $\alpha = 1, \beta = 0.001, \rho = 0.01$, and (d) $\alpha = 4, \beta = 0.04, \rho = 0.01$.

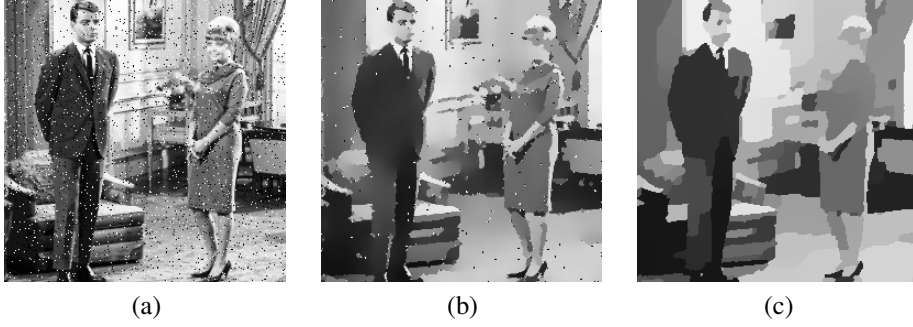


Figure 4: Segmentation of a noisy image degraded with 5% salt and pepper noise. (a) Source image. (b) Reconstruction using AT model. (c) Reconstruction using Shah's modified functional (both results are obtained with $\alpha = 1$, $\beta = 0.01$, $\rho = 0.01$).

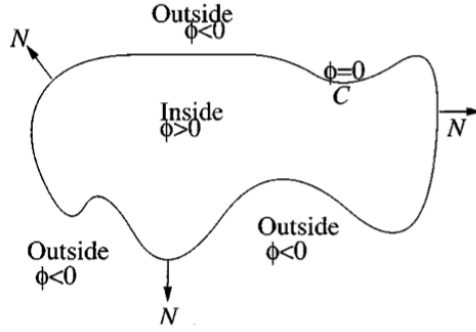


Figure 5: A curve can be represented as the zero-level line of a level set function (image taken from [4]).

and $\phi < 0$, respectively. Thus, the CV model can be seen as a two-phase piecewise constant approximation of the MS model, which can theoretically be obtained by letting the weight α of the smoothness term tend to infinity, and forcing a two-region segmentation.

To segment a given image, the functional (17) needs to be minimized with respect to c_1 , c_2 , and ϕ . Keeping ϕ fixed, the average gray values c_1 and c_2 can be easily estimated by

$$(19) \quad c_1 = \frac{\int_{\Omega} f(x)H(\phi(x))dx}{\int_{\Omega} H(\phi(x))dx},$$

$$(20) \quad c_2 = \frac{\int_{\Omega} f(x)(1 - H(\phi(x)))dx}{\int_{\Omega} (1 - H(\phi(x)))dx}.$$

Keeping c_1 and c_2 fixed and using the calculus of variations for the functional (17), the gradient descent equation for the evolution of ϕ is derived as

$$(21) \quad \frac{\partial \phi}{\partial t} = \delta(\phi) \left[\mu \nabla \cdot \left(\frac{\nabla \phi}{|\nabla \phi|} \right) - \lambda_1 (f - c_1)^2 + \lambda_2 (f - c_2)^2 \right].$$

In Figure 6, we illustrate segmentation of a sample noisy image which contains several objects of different shapes and sizes. We initialize the level set function ϕ with $\phi_0 = -\sqrt{(x-100)^2 + (y-100)^2} + 90$. As the zero-level line of the evolving level set function ϕ is attracted to object boundaries, a more accurate piecewise constant approximations of the original image f is recovered. Although some of the objects in the image have holes, they can be automatically detected by the CV model without considering additional curves since the level set formulation allows change of topology.

Numerical Implementation

In the numerical approximation of the CV model, generally, a regularized Heaviside function is used. For the remainder of this thesis, the following regularization is considered:

$$(22) \quad H_\varepsilon(z) = \frac{1}{2} \left(1 + \frac{2}{\pi} \arctan \left(\frac{z}{\varepsilon} \right) \right),$$

$$(23) \quad \delta_\varepsilon(z) = \frac{dH_\varepsilon(z)}{dz} = \frac{1}{\pi} \frac{\varepsilon}{\varepsilon^2 + z^2}.$$

The evolution equation of ϕ (21) can be discretized by using standard finite differences as

$$(24) \quad \begin{aligned} \frac{\phi_{i,j}^{k+1} - \phi_{i,j}^k}{\Delta t} = & \delta(\phi_{i,j}^k) \left[\mu \Delta_-^x \cdot \left(\frac{\Delta_+^x \phi_{i,j}^{k+1}}{\sqrt{(\Delta_+^x \phi_{i,j}^k)^2 + (\phi_{i,j+1}^k - \phi_{i,j-1}^k)^2 / 4}} \right) \right. \\ & + \mu \Delta_-^y \cdot \left(\frac{\Delta_+^y \phi_{i,j}^{k+1}}{\sqrt{(\phi_{i+1,j}^k - \phi_{i-1,j}^k)^2 / 4 + (\Delta_+^y \phi_{i,j}^k)^2}} \right) \\ & \left. - \lambda_1 (f_{i,j} - c_1(\phi^k))^2 + \lambda_2 (f_{i,j} - c_2(\phi^k))^2 \right] \end{aligned}$$

where (i, j) denotes the pixel position, Δt is the time step, and forward and backward differences are defined as

$$\begin{aligned} \Delta_-^x \phi_{i,j} &= \phi_{i,j} - \phi_{i-1,j}, & \Delta_+^x \phi_{i,j} &= \phi_{i+1,j} - \phi_{i,j}, \\ \Delta_-^y \phi_{i,j} &= \phi_{i,j} - \phi_{i,j-1}, & \Delta_+^y \phi_{i,j} &= \phi_{i,j+1} - \phi_{i,j}. \end{aligned}$$

The minimization procedure is summarized in Algorithm 2. Keeping ϕ fixed, first the average gray values of object and background regions c_1 and c_2 are estimated. Next, the level set function ϕ is evolved according to (24). A numerical stopping criteria can be defined in the sense that the rate of change of ϕ or the overall energy (17) is less than a threshold.

REFERENCES

- [1] L. Ambrosio and V. Tortorelli. On the approximation of functionals depending on jumps by elliptic functionals via Γ -convergence. *Commun. Pure Appl. Math.*, 43(8):999–1036, 1990.

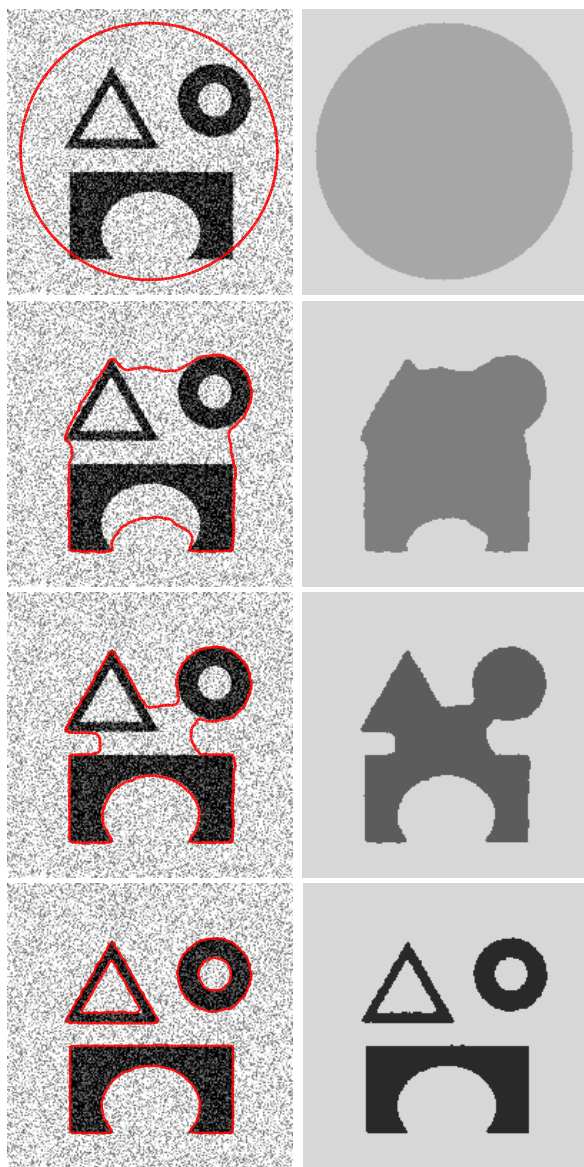


Figure 6: Example segmentation results (evolving contour ϕ superimposed on the original image f and the corresponding piecewise constant approximations of f). The parameters and the initial level set function are chosen as $\lambda_1 = \lambda_2 = 1$, $\mu = 0.5 \cdot 255^2$, $\varepsilon = 1$, and $\phi_0 = -\sqrt{(x - 100)^2 + (y - 100)^2} + 90$.

Algorithm 2 Minimization of the Chan-Vese Model

- 1: Initialize the level set function with $\phi^0 = \phi_0$
 - 2: **for** $k = 0$ to $kmax$ **do**
 - 3: Estimate $c_1(\phi^k)$ and $c_2(\phi^k)$ using (19) and (20), respectively
 - 4: Solve (24) for ϕ^{k+1}
 - 5: Check whether a numerical stopping criteria on ϕ is reached
 - 6: **if** it is reached **then**
 - 7: stop iterations
 - 8: **end if**
 - 9: **end for**
-

- [2] A. Braides. *Approximation of Free-Discontinuity Problems*. Lecture Notes in Mathematics, Vol. 1694. Springer-Verlag, 1998.
- [3] T. Chan and L. Vese. Variational image restoration and segmentation models and approximations. *UCLA CAM-report 97-47*, September 1997.
- [4] T. F. Chan and L. A. Vese. Active contours without edges. *IEEE Trans. Image Processing*, 10(2):266–277, 2001.
- [5] J. P. Kaufhold. *Energy Formulations of Medical Image Segmentations*. PhD thesis, Boston University College of Engineering, Department of Biomedical Engineering, Boston, MA, 2000.
- [6] D. Mumford and J. Shah. Optimal approximations by piecewise smooth functions and associated variational problems. *Commun. Pure Appl. Math.*, 42(5):577–685, 1989.
- [7] S. Osher and J. A. Sethian. Fronts propagating with curvature-dependent speed: Algorithms based on Hamilton-Jacobi formulation. *J. Comput. Phys.*, 79:12–49, 1988.
- [8] J. Sethian. *Level Set Methods*. Cambridge University Press, 1996.
- [9] J. Shah. A common framework for curve evolution, segmentation and anisotropic diffusion. In *CVPR*, pages 136–142, 1996.